Desalination 500 (2021) 114886

Contents lists available at ScienceDirect

Desalination

journal homepage: www.elsevier.com/locate/desal

Combined electrocoagulation-microfiltration-membrane distillation for treatment of hydraulic fracturing produced water

Mahmood Jebur [a,g], Yu-Hsuan Chiao [a], Kupaaikekaiao Thomas [b], Tanmoy Patra [c], Yuhe Cao [a,*], Kyunghoan Lee [d], Nicholas Gleason [d], Xianghong Qian [c], Yunxia Hu [e], Mahdi Malmali [f], S. Ranil Wickramasinghe [a,*]

[a] Ralph E Martin Department of Chemical Engineering, University of Arkansas, Fayetteville, AR 72701, United States
[b] Chemical and Biological Engineering, University of Colorado Boulder, Boulder, CO 80309, United States
[c] Department of Biomedical Engineering, University of Arkansas, Fayetteville, AR 72701, United States
[d] Department of Science and Mathematics, Northwest Arkansas Community College, Bentonville, AR 72712, United States
[e] State Key Laboratory of Separation Membranes and Membrane Processes, National Center for International Research on Membrane Science and Technology, School of Materials Science and Engineering, Tianjin Polytechnic University, Tianjin 300387, PR China
[f] Department of Chemical Engineering, Texas Tech University, Lubbock, TX 79409, United States
[g] Department of Chemical Engineering, Tikrit University, Tikrit, Salah Al-din, Iraq

HIGHLIGHTS

- Combined EC-MF-MF process can treat produce water with TDS as high as 245,300 mg L^{-1}.
- Electrocoagulation used to flocculate organic compounds and particulate matter.
- Microfiltration rapidly removes flocculated matter.
- Membrane distillation desalinates PW.
- Three different membranes with different surface properties and morphologies tested.

GRAPHICAL ABSTRACT

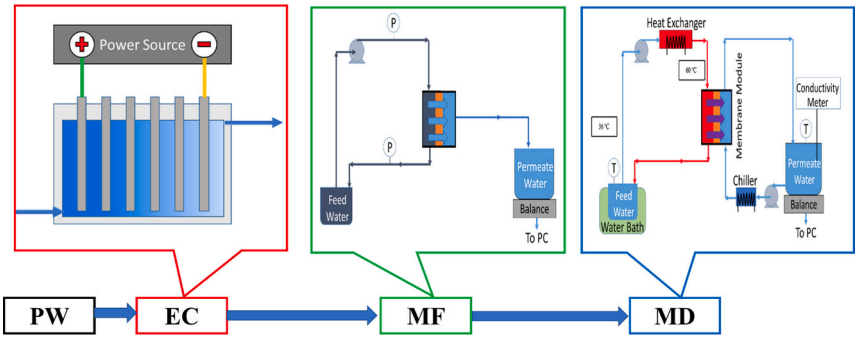

ARTICLE INFO

Keywords:
Carbon nanotube
Direct contact membrane distillation
Electrospun membrane
Fouling
Wastewater

ABSTRACT

Hydraulic fracturing flowback and produced water is a highly impaired wastewater containing dissolved salts polar and non-polar organic compounds, oil and surfactants. Here a combined electrocoagulation - microfiltration – membrane distillation process has been used to treat this wastewater. Electrocoagulation followed by microfiltration was used to pretreat the wastewater prior membrane distillation. The initial total dissolved solids (TDS) concentration was extremely high being 245,300 mg L^{-1}. After electrocoagulation, the total organic carbon (TOC) was reduced from 120 mg L^{-1} to 64 mg L^{-1}. Tangential flow microfiltration using a 0.1 μm pore size polyethersulfone membrane was used to separate the particulate matter after electrocoagulation and to further reduce the TOC to 44 mg L^{-1}. Membrane distillation was used to desalinate the pretreated produced water resulting in a high quality treated water (TDS of 56 mg L^{-1} and TOC 1 mg L^{-1}). Three membranes with

* Corresponding authors at: Ralph E. Martin Department of Chemical Engineering, University of Arkansas, Fayetteville, AR, United States.
E-mail addresses: mgjebur@uark.edu (M. Jebur), yuhecao@uark.edu (Y. Cao), swickram@uark.edu (S.R. Wickramasinghe).

https://doi.org/10.1016/j.desal.2020.114886
Received 28 May 2020; Received in revised form 22 November 2020; Accepted 26 November 2020
Available online 17 December 2020

very different surface morphology were used: commercially available polyvinylidene fluoride, electrospun poly (vinylidene fluoride-*co*-hexafluoropropylene) nanofibers and multiwalled carbon nanotube coated polytetrafluoroethylene.

The TDS in the retentate increased to over 350,000 mg L^{-1}. During membrane distillation, the temperature of the feed tank was maintained at 36 °C while the feed entered the module at 60 °C in order to minimize scaling on the membrane. The surface properties of an ideal membrane that is resistant to wetting and provides high flux is likely to depend on the TDS and properties of the wastewater.

1. Introduction

Water that is co-produced during oil and gas production, known as produced water (PW), is a major waste stream. The United States produces about 21 billion barrels of PW per year [1]. The amount of PW that is generated depends on the geological formation and the type of energy resource being developed. Here we focus on hydraulic fracturing and horizontal drilling which has enabled the recovery of oil and gas from shale and other tight rock formations [2]. However, this technology requires the use of a large amount of water [3].

Treating hydraulic fracturing flowback and co-produced water referred to here collectively as PW is very challenging and expensive. Fracking fluid is pumped into the well at high pressure in order to fracture the rock formation [4–6]. The fracking fluid consists of 98% water and sand. However, a number of chemicals such as friction reducers, surfactants, corrosion inhibitors and flow improvers are added [7]. After fracturing the rock formation, the pressure is reduced, and the fracking water flows back to the surface with oil/gas and co-produced water [3].

The composition of the PW water depends on the geological formation where it is trapped. In general, the PW contains high concentrations of dissolved salts referred to as total dissolved solids (TDS). In addition, there are dissolved polar and nonpolar organic compounds (total organic carbon, TOC), as well as oil, grease, fuels and additives associated with the fracking fluids that make up the total suspended solids (TSS) [1,8].

Partially treating PW onsite or transporting PW to a centralized water treatment facility is the most common practice in United States. Recycling and reusing PW from hydraulic fracturing operations is essential to preserve water resources and manage wastewater disposal. Most often the PW is transported to a deep well injection site where it is injected deep underground into a geologically isolated formation. Nevertheless, the PW could escape from the formation and contaminate surface or groundwater [2]. Further the United States Geological Survey (USGS) found that deep-well injection is the main cause of earthquakes, not the hydraulic fracturing process itself [9]. New technologies for treating PW from hydraulic fracturing operations in an affordable manner are necessary.

Once the PW is recovered it is treated using a number of different unit operations which can be divided into three treatment stages [10]. Primary separation treats the water sufficiently for deep well injection. Secondary separation units treat the water for reuse to stimulate new wells. Finally, tertiary separation operations treat the water for discharge into lakes and rivers etc. The aim of this work is to develop a combined primary, secondary and tertiary treatment process for PW using membrane-based separation processes.

All membrane-based separation processes suffer from fouling. This is particularly problematic for PW from hydraulic fracturing operations as it contains dissolved organic and inorganic compounds as well as surfactants and other low surface tension compounds [11–13]. Rejected species will accumulate in the membrane pores and on the membrane surface, which compromises performance.

Common primary and secondary treatment processes consist of chemical precipitation and dissolved air flotation or electrocoagulation (EC) followed by media filtration. Here we use EC as the primary unit operation. EC is an alternative to chemical coagulation. EC can effectively remove organic compounds and other contaminants by generation of an electrical current which leads to dissolution of a metal electrode such as aluminum or iron [14].

The setup of an EC system includes metal anode(s) and cathode(s) placed inside the EC cell which contains the PW. Multiple reactions occur simultaneously in the feed PW. Metal ions are driven from the anode to the water. Water is hydrolyzed on the surface of the cathode creating hydrogen gas and hydroxide ions. The hydrogen gas bubbles rise up in the solution while the metal ions and hydroxide ions react to create metal-hydroxide complexes [15]. These metal complexes can polymerize and trap organic compounds and suspended particles. Some of the aggregated particles sink to the bottom of the system forming a sludge. EC is already used by companies such as Haliburton [16] and Baker Hughes [17]. Use of EC can lead to a more easily disposable sludge reducing disposal costs [10]. Further we have combined EC with forward osmosis and membrane distillation (MD) in the past [18,19] and shown that it is effective at reducing the TOC of the feed which suppresses membrane fouling.

Numerous unit operations are used as secondary treatment processes such as filtration and oxidation. Here we use microfiltration (MF). In our earlier work [18,19] after EC we allowed the flocs to sediment. We then recovered the supernatant water and desalinated it using forward osmosis or MD or a combination of both unit operations [20]. However, sedimentation times could be as long as 24 h which is impractical. In addition, low pressure membrane processes such as microfiltration are attractive as they can remove particulate matter as well as microorganisms.

Typically, thermal desalination technologies are used as the tertiary treatment process. Due to the very high TDS of the PW, pressure driven membrane desalination processes such as reverse osmosis and nanofiltration are not commonly used. Here we use MD to desalinate the PW. MD is an emerging membrane-based technology that could find applications in the treatment of highly impaired brackish wastewater. It is a thermally driven separation process that makes use of a hydrophobic membrane. Consequently, only vapor molecules (water and volatile species that are dissolved in the PW) are able to pass through the membrane [21]. Here, we have investigated direct contact membrane distillation. The hot feed flows on one side of the membrane. The membrane is a thermal insulator as well as a physical barrier between the hot feed and the cold permeate (distillate). The feed and permeate streams are in direct contact with the membrane [22,23].

MD is attractive for treatment of high TDS wastewater as very high rejection of dissolved salts and nonvolatile species is possible. While the feed temperature must be elevated compared to the permeate temperature the feed need not be at its boiling point as is the case with thermal distillation. MD can take advantage of the low-grade waste heat that is produced at industrial sites [20]. All that is needed is a vapor pressure difference between the feed and permeate sides of the membrane ensuring passage of water vapor from the feed to the permeate. However, since the MD membrane is hydrophobic, it has a poor resistance to hydrophobic foulants due to hydrophobic-hydrophobic interactions. Dissolved organic compounds, surfactants and low surface tension compounds containing hydrophobic functional groups can easily adsorb on the membrane. In order to mitigate membrane fouling we propose a combined EC-MF process to pretreat the PW prior to MD, which can extend membrane life.

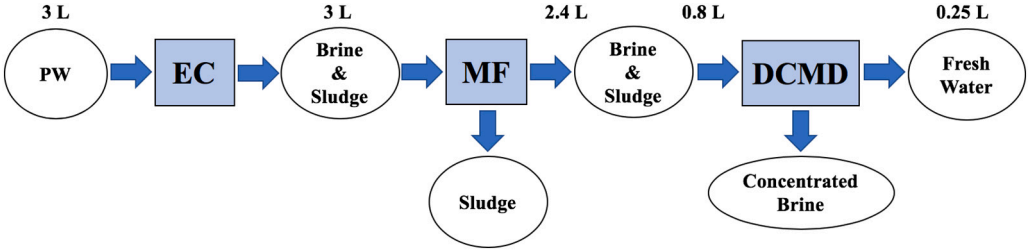

Fig. 1. Diagram of the combined EC-MF-MD process investigated here.

Fig. 1 shows the concept of a combined EC-MF-MD processes for PW treatment. In this work the process was operated in batch mode. EC leads to flocculation of much of the contaminants (suspended solids and insoluble organic compounds) into a sludge. The volume of PW treated was 3 L. Next the EC treated PW was immediately filtered using MF to separate the brine from the sludge. As indicated in Fig. 1, 3 L of treated PW resulted in about 0.6 L of sludge and 2.4 L of filtered brine. Finally, MD is used to desalinate the brine. Each MD run consisted of a feed volume of 0.8 L. For a feed volume of 0.8 L about 0.25 L of water was recovered.

In this work, three different MD membranes were evaluated using the EC-MF-MD process developed here: a commercially available polyvinylidene fluoride (PVDF) membrane, an electrospun *co*polymer membrane consisting of poly(vinylidene fluoride-*co*-hexafluoropropylene) (PVDF-HFP) and multiwalled carbon nanotube (MWCNT) coated polytetrafluoroethylene (PTFE) membrane. The three membranes had different morphologies and surface properties. The focus of this study was to evaluate the combined EC-MF-MD processes for treating real PW and to understand the effects of water quality and operating conditions on fouling and scaling of three different MD membranes.

2. Materials and methods

2.1. PW characterization

PW was obtained from a hydraulic fracturing facility in Texas, USA. Prior to testing the water was analyzed at the Arkansas Water Resources Center, University of Arkansas (Fayetteville, AR, USA). Total dissolved solid (TDS), total suspended solids (TSS), turbidity and total organic carbon (TOC) were measured using EPA standard methods 160.1, 160.2, 415.1 and 180.1 [24], respectively. Cations and anions were measured using EPA method 200.7 and 300.0, respectively [25]. Conductivity was measured using a conductivity meter (VWR, Radnor, PA).

2.2. Materials

Acetone and *N*,*N*-dimethylacetamide (DMAc) were purchased from Alfa-Aesar (Ward Hill, MA, USA). Deionized (DI) water used throughout the investigation was collected from Thermo Fisher 18 MΩ Barnstead Smart2Pure system (Schwerte, Germany). Sodium hydroxide and PVDF-HFP were purchased from Sigma Aldrich (St. Louis, MO, USA). Commercial PVDF membranes were obtained from MilliporeSigma (Billerica, MA, USA). PTFE membranes were purchased from Shengju Environmental Science and Technology Co., Ltd. (Hangzhou, China). Multi-walled carbon nanotubes (MWCNTs) were purchased from Chengdu Organic Chemicals Co. Ltd. (Chinese Academy of Sciences, Chengdu, China). The MWCNTs have a diameter of ~8 nm, a length of 10– 20 μm, and purity ~98%. Mineral oil was obtained from Walmart Inc. (Bentonville, AR, USA).

2.3. Fabrication of electrospun membranes

The solvent used was a 7:3 (wt%) acetone: DMAc solution. The PVDF-HFP was dried at 70 °C overnight then dissolved under mixing (200 rpm) at a temperature of 45 °C in the solvent to form a 10 wt% polymer solution. The homogeneous polymer solution was placed in a fume hood overnight for degassing. A diagram of the electrospinning system is shown in Fig. 2. The polymer solution was ejected from a syringe at a specified flow rate. The needle was connected to a high voltage supply. The rotating collector was grounded. The distance between the needle and the rotating collector was 15 cm. The electrospun membranes were fabricated at 23 °C and 50% relative humidity.

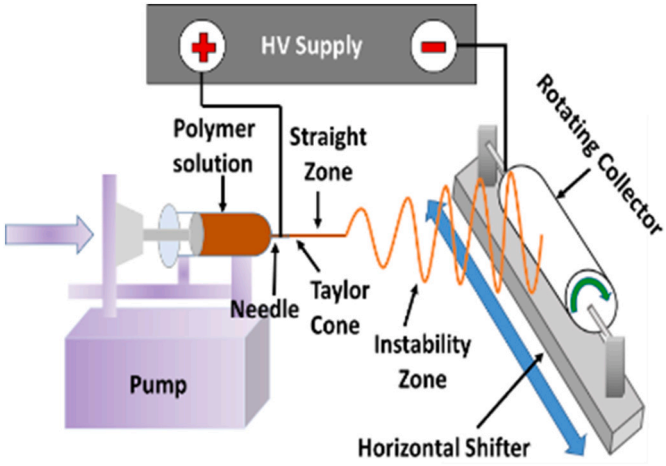

Fig. 2. Diagram of electrospinning set up.

Briefly, a droplet sits at the end of the needle and is slowly pushed by the plunger. The liquid becomes charged due to the electric field between the tip of the needle and the collector plate. A Taylor cone forms. The droplet stretches and a jet erupts from the cone at the critical point where electrostatic repulsion overcomes the surface tension of the liquid. The jet heads for the point with a lower potential (the collector plate). The solvent evaporates as the jet reaches the collector plate. The jet does not break up as the polymer chains are entangled. The mat that forms at the collector is a distribution of continuous nanofibers [26,27]. The electrospinning conditions were as follows: voltage 16 kV, flow rate 1 mL/h, collector rotation speed 90 rpm, spinning time 10 h. After electrospinning, the membranes were dried in a fume hood for 24 h to remove the residual solvent. Then the electrospun membranes were subjected to 3 min hot-press post treatment at 130 °C to further remove solvent and improve stability.

2.4. Fabrication of the MWCNT-coated membrane

An ethanol dispersion of 0.4 g L^{-1} MWCNTs was prepared immediately before coating the PTFE membrane. MWCNTs were dissolved in ethanol for 10 min. The suspension was stirred at 100 rpm using a magnetic stirrer followed by sonication for 2 h using a probe sonicator (JY 92-IIDN, Scientz, Ningbo, China) at room temperature. Spray coating was conducted using a spray gun (LPH-50-S9, Anestiwata,

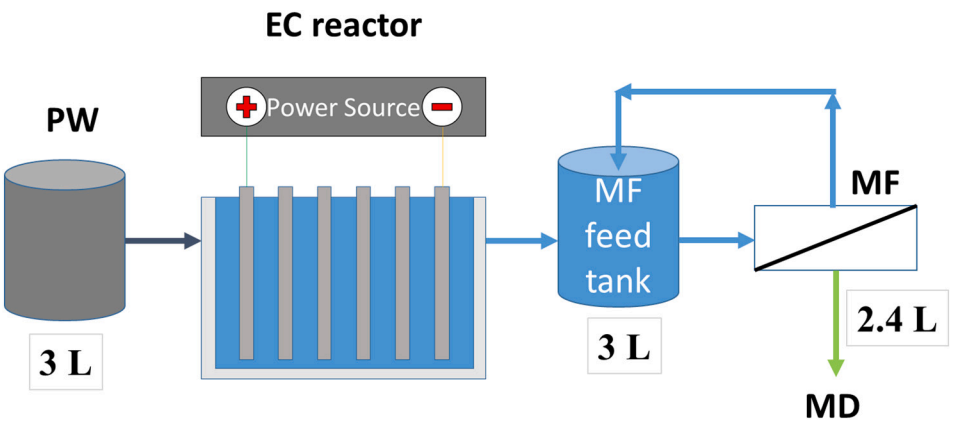

Fig. 3. Diagram showing combined EC-MF system investigated here.

Yokohama, Japan) having a nozzle size of 0.8 mm at a pressure of 1 bar. The distance between the nozzle and the membrane was 20 cm. After spraying, the MWCNT-coated membrane was dried at 50 °C in an oven for 1 h. Then, the MWCNT-coated membrane was heat-treated in air at 250 °C for 2 h in a muffle furnace to firmly bind the MWCNTs and substrate.

2.5. Membrane characterization

The mean pore diameter on the membrane surface and the thickness of skin layer were measured using Nano Measure software based on the scale bar in the SEM images. For each set of data, more than 50 pores were randomly selected from the SEM images of three individual parallel specimens [28]. Liquid entry pressure (LEP) was determined as described by Smolder and Franken [29]. A Sterlitech HP4750 (Kent, WA) stainless steel cell was filled with deionized (DI) water and pressurized to 13.8 kPa. Then the feed pressure was gradually increased at 13.8 kPa/min. When a continuous flow of DI water through the membrane was first observed and the pressure was recorded as the LEP [30].

A sessile drop contact angle goniometer (Model 100, Rame-Hart Instrument Company, Netcong, NJ, USA) was used to measure membrane static water and oil contact angles. For the water contact angle, the volume of the DI water droplet was 2 μL which was introduced at a rate of 0.5 μL/s. For the oil contact angle, the underwater oil (mineral oil) droplet volume was 5 μL which was introduced at a rate of 0.5 μL/s. Both water and oil contact angles were measured after allowing the droplet to stabilize for 10 s. The contact angle measurement for each membrane was obtained at three different locations and the average value is reported.

Both scanning electron microscopy (SEM) and energy-dispersive X-ray (EDX) spectroscopy were used to determine the surface morphology and elemental analysis, respectively, for each membrane before and after MD using Nova Nanolab 200 Duo-Beam Workstation (FEI, Hillsboro, OR, USA). Atomic force microscopy (AFM) images were acquired using Bruker Dimension icon instrument (Santa Barbara, CA, USA) to obtain detailed information on the surface roughness. AFM tapping mode was conducted using Antimony-loaded Si-based probes. AFM images were obtained for membranes before and after MD.

2.6. EC MF pretreatment

A diagram of the combined EC-MF system is shown in Fig. 3. A custom-built polycarbonate reactor having dimensions of 4 cm × 32 cm × 40 cm with a total volume of 5120 cm^3 was used to conduct all the EC experiments. Six aluminum electrodes were fitted vertically inside the reactor with a 5 mm inter-electrode spacing and a total effective surface area of 3760 cm^2. A DC power supply (Hewlett Packard, Palo Alto, CA, USA) was connected to a reverse polarity switch which enabled the direction of the current to alternate every 30 s. This is essential to prevent formation of a passivation layer on the electrode which would suppress further reactions [31,32].

Immediately after EC, microfiltration was conducted using a custom-built MF cell developed in previous work [33]. The entire 3 L of EC treated feed water was placed in the MF feed tank. Initially the permeate

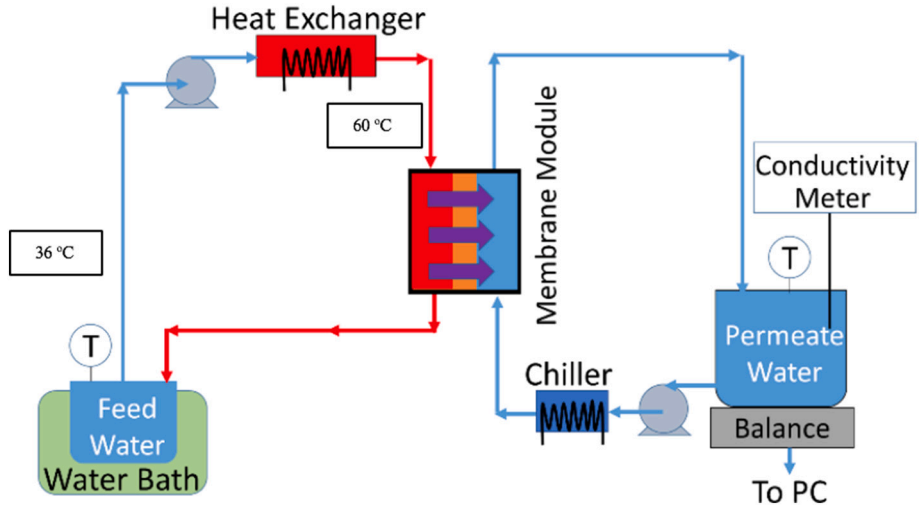

Fig. 4. Diagram of MD system investigated here.

Table 1
Water quality analysis for PW received from the hydraulic fracturing facility and after each water treatment operation.

Parameter	Unit	PW	PW treated by EC	PW treated by EC-MF	PW treated by EC-MF-MD
TDS	mg L^{-1}	245,300	238,400	239,760	56
TOC	mg L^{-1}	120	64	44	1
TSS	mg L^{-1}	131	186	48	1
Turbidity	NTU's	6	13	0.3	0.4
pH	–	6.7	3.8	3.9	7.1
Chloride	mg L^{-1}	156,820	160,250	166,170	5
Sulfate	mg L^{-1}	478	419	430	0
Iron	mg L^{-1}	0.2	0.6	0.7	0
Boron	mg L^{-1}	97	87	85	0
Calcium	mg L^{-1}	30,500	30,300	31,700	1
Magnesium	mg L^{-1}	5454	5500	5335	0
Manganese	mg L^{-1}	0.1	0.3	0.4	0
Nickel	mg L^{-1}	0.2	0.4	0.4	0
Potassium	mg L^{-1}	4331	4800	4680	0.4
Aluminium	mg L^{-1}	0	97	64	0
Sodium	mg L^{-1}	63,600	68,600	68,100	4
Conductivity	µS/cm	323,400	228,000	229,000	35

outlet was closed and feed was recirculated through the membrane module by means of a diaphragm pump (P800, King-Kong, Taiwan). The membrane surface area available for filtration was 33.75 cm^2. The feed flow rate was 1.8 L min^{-1} and the feed pressure was 110 kPa. The permeate side pressure was essentially at atmospheric pressure. Once steady state had been reached, the permeate outlet was opened and permeate was collected in the permeate tank which was placed on a computer-connected analytical balance (Mettler Toledo, Columbus, OH). The permeate flux was calculated based on the rate of permeate collection in the permeate tank. About 80% of the EC treated water was recovered (see Fig. 1). After each cycle, the membrane was cleaned by circulating DI water for 1 h prior to starting a new cycle. A commercially available PES membrane purchased from Membrane Science Inc. (Hsinchu, Taiwan) and having a porosity of 80.4%, 0.1 µm pore size and 43.7° air contact angle was used.

2.7. MD

A diagram of the MD system is shown in Fig. 4. A custom-made acrylic membrane cell with 40 cm^2 effective membrane area and 2 mm deep channels was used as the membrane module. PTFE spacers (ET 8700, Industrial Netting, Minneapolis, MN, USA) were used for mechanical support and mixing. Feed and permeate streams were pumped on opposite sides of the membrane at 0.05 L min^{-1} using two peristaltic pumps (Masterflex I/P, Cole Parmer, Vernon Hills, IL) in counter current flow. The weight of the permeate was measured and recorded by a computer-connected analytical balance (Mettler Toledo, Columbus, OH, USA). The temperature of the permeate tank was maintained at 20 °C using an external chiller (PolyScience, Niles, IL, USA). The feed tank was placed in a water bath to maintain the temperature at 36 °C. The feed water was pumped through a heat exchanger in order to increase the temperature of the feed entering the MD module to 60 °C. From our previous work, we found that cooling the feed tank relative to the temperature of the feed entering the MD module induces precipitation in the feed tank and suppresses scale formation on the membrane surface due to supersaturation of the feed. In this way we increase water recovery and limit scale formation on the membrane surface [34].

Table 2
Bulk membrane properties.

Membrane	Thickness (µm)	Mean pore size (µm)	LEP (kPa)	Water contact angle (°)	Oil contact angle (°)
Commercial PVDF	103 ± 5	0.45	233.7	144.6 ± 3	71.8 ± 2
Electrospun PVDF-HFP	100 ± 7	0.60	155.1	137.7 ± 1	82.8 ± 1
MWCNT PTFE	63 ± 1	0.21	96.5	150.0 ± 4	33.7 ± 3

The water flux was calculated based on the weight change of the permeate tank. The permeate conductivity was continuously monitored using a conductivity meter (VWR, Radnor, PA, USA). Each MD experiment was conducted using 800 ml of pretreated PW. It was assumed that pore wetting and membrane failure occurred once the permeate conductivity increased above 50 µS cm^{-1}. A regeneration cycle was conducted once the permeate conductivity reached 50 µS cm^{-1} or there was no weight increase of the permeate for 20 min. Regeneration of the membrane involved pumping DI water on both sides of the membrane at 0.5 L min^{-1} for 1 h.

3. Results and discussion

3.1. Wastewater characterization

Prior to receival the PW was treated with chlorine dioxide at the hydraulic fracturing facility. Table 1 shows the water quality parameters of the PW as received from the hydraulic fracturing facility as well as after each treatment step. As can be seen the TDS is very high, being about 7 times more than seawater. The majority of the inorganic ions present are chlorine, calcium, magnesium potassium and sodium. A high concentration of calcium ions (30,500 mg L^{-1}) can potentially lead to membrane scaling due to the precipitation of calcium sulfate [20]. The TOC and TSS are 120.0 mg L^{-1} and 131 mg L^{-1}, respectively. The water is highly impaired. It is important to note that the quality of the PW in general is highly variable, and this will affect the efficiency of the treatment operations. By comparison with previous studies [18,20,25,35], this PW contains much higher TDS. The percent difference (electroneutrality) between the sum of the cations and anions was 4.1% indicating that the analysis of the PW is of sufficient accuracy.

3.2. Membrane characterization

3.2.1. Bulk membrane properties

Table 2 lists the characteristics of the MD membranes, including mean pore size, thickness, contact angle and LEP. As can be seen all three membranes have a large water contact angles and are hydrophobic. This is essential for MD as only water vapor should pass through the membrane pores. The membrane should be resistant to wetting by water. However, Table 1 suggests that the dissolved organic compounds present in PW could adsorb on the membrane surface. If these compounds are polar, they could lead to scale deposition on the layer of adsorbed organic compounds [18]. Consequently, an oleophobic membrane surface is desirable. As indicated by Table 2, the electrospun membrane has the highest oil contact angle.

3.2.2. SEM images

SEM images of all three membranes before and after MD are given in Fig. 5. Fig. 5A, B and C are for commercial PVDF, electrospun PVDF-HFP and MWCNT PTFE membranes before MD. Fig. 5D, E and F are for

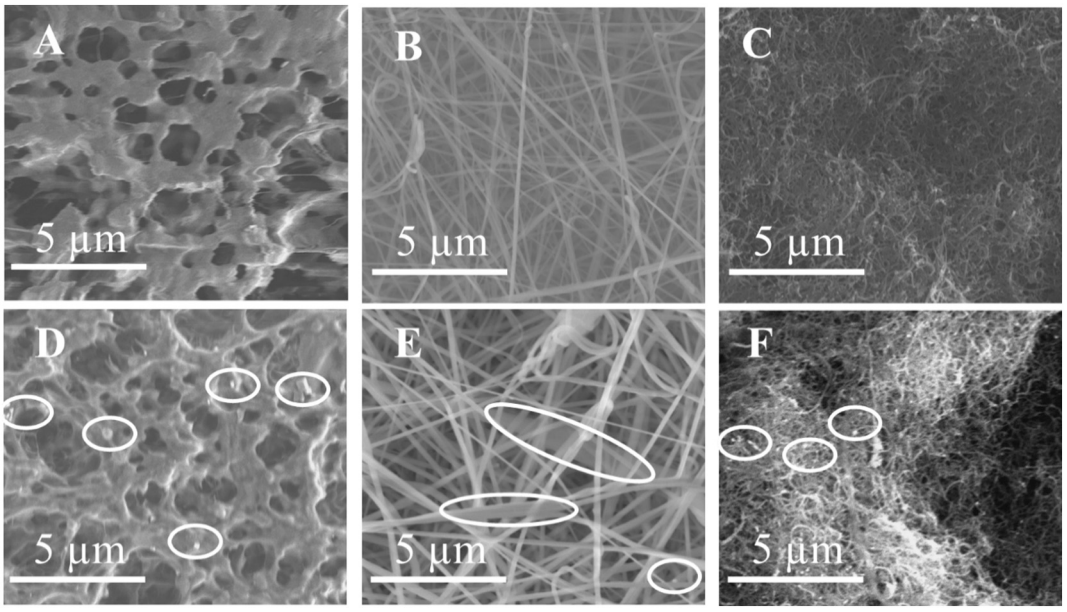

Fig. 5. SEM images of the membrane surface before and after MD: 5A, 5B 5C are for commercial PVDF, electrospun PVDF-HFP and MWCNT PTFE membranes before MD and 5D, 5E, 5F are after MD.

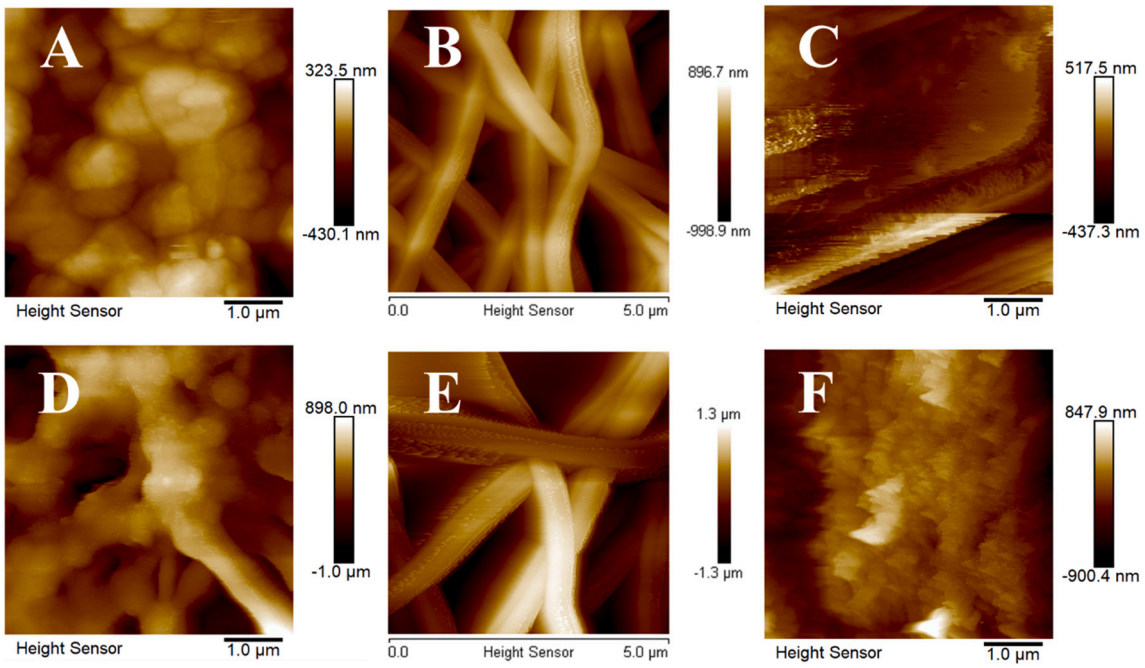

Fig. 6. AFM images (A, B and C) for commercial PVDF, electrospun PVDF-HFP and MWCNT PTFE membranes before MD. Images D, E and F are for commercial PVDF, electrospun PVDF-HFP and MWCNT PTFE membranes after MD.

commercial PVDF, electrospun PVDF-HFP and MWCNT PTFE membranes after MD. As can be seen some deposition (highlighted with circle) on the membrane surface is observed after MD.

3.2.3. AFM images

The surface morphology of the membranes before and after MD was imaged by AFM as shown in Fig. 6. Average roughness values are given in Table 3. As can be seen the surface pore morphology changes for all three membranes after MD. In addition, Table 3 indicates an increase in surface roughness after MD for all membranes.

3.2.4. EDX results

The EDX spectra of commercial PVDF, electrospun PVDF-HFP and MWCNT PTFE membranes before and after MD are given in Fig. 7. The average elemental ratios of carbon/fluorine (C/F) and oxygen/fluorine (O/F) for all three membranes before and after MD are given in Table 3. As can be seen the C/F and O/F ratios of all the membranes increased after MD, which is mainly due to the organic fouling.

3.3. EC performance

In the presence of an aluminum electrode, the main electrode

Table 3
Average roughness and C/F and O/F atomic percent ratios for the three membranes before and after MD.

Membranes	Average roughness Ra (nm)		C/F atom percental ratio		O/F atom percental ratio	
	Before MD	After MD	Before MD	After MD	Before MD	After MD
Commercial PVDF	77	236	2.21	3.36	0.17	0.35
Electrospun PVDF-HFP	275	404	1.61	2.32	0.08	0.14
MWCNT PTFE	89	202	3.45	21.79	0.10	1.28

reactions that occur are as follows [36].

At the anode:

$$Al \rightarrow Al^{3+} + 3e^{-} \quad (1)$$

At the cathode:

$$2H_2O + 2e^{-} \rightarrow H_2 + 2OH^{-} \quad (2)$$

In the solution:

$$Al^{3+} + H_2O \rightarrow AlOH^{2+} + H^{+} \quad (3)$$

$$AlOH^{2+} + H_2O \rightarrow Al(OH)^{+}{}_2 + H^{+} \quad (4)$$

$$Al(OH)^{+}{}_2 + H_2O \rightarrow Al(OH)^{0}{}_3 + H^{+} \quad (5)$$

$$Al(OH)^{0}{}_3 + H_2O \rightarrow Al(OH)^{-}{}_4 + H^{+} \quad (6)$$

During EC, the aluminum ions are generated continuously at the anode. The reduction of water takes place at the cathode forming hydroxide ions. In the solution, a variety of aluminum hydroxides are produced when coagulating ions (aluminum and/or hydroxide ions) undergo hydrolysis in water. Reactions (3)–(5) are the dominant reactions at pH 6.7, the pH of the PW. Introducing aluminum hydroxides can help destabilize suspended, emulsified and dissolved contaminants, which can further aggregate and precipitate as sludge or lift up to the surface as flocs. Soluble organic compounds can be adsorbed by the aggregated aluminum hydroxides. This adsorption phenomenon is a result of the liquid-solid intermolecular attraction forces between the adsorbable solute in the solution and the large surface area of the porous floc that form.

The bipolar series (BPS) configuration was used in this work because only the first and last electrodes are connected to the power supply, simplifying the electrical connections (see Fig. 3). Further previous studies indicated that using BPS configuration can enhance the TOC removal [37]. Initial experiments focused on determining an appropriate EC current and reaction time. A range of currents (1 to 9.5 A) and reaction times of 5 min and 20 min were studied. Each EC experiment was conducted using 600 mL of PW. After EC, the treated water was allowed to sediment for 6 h. Treated water was removed from the sludge and settled floc. The TOC removal for the recovered water was defined as,

Table 4
Percentage removal of TOC for different currents and reaction times.

EC operating conditions	% TOC removal
1 A, 5 min	17.9
5 A, 5 min	29.3
8 A, 20 min	46.4
9.5 A, 20 min	48.45

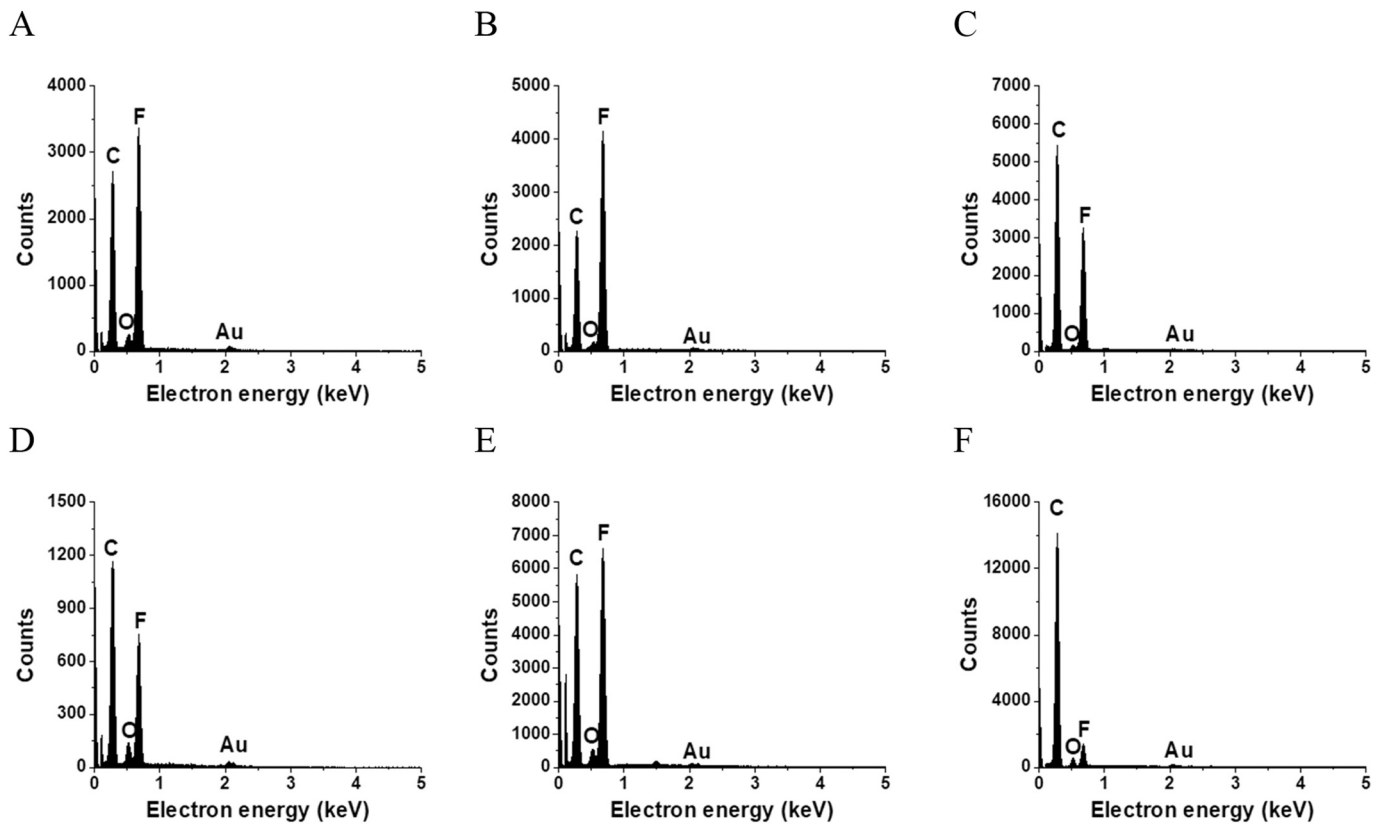

Fig. 7. EDX spectra of the membrane surface before and after MD: A, B, and C are for commercial PVDF, electrospun PVDF-HFP and MWCNT PTFE membranes, respectively, before MD and D, E, and F are after MD.

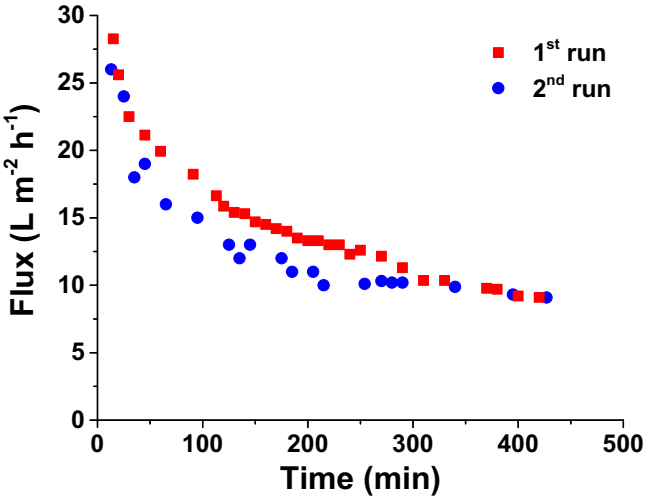

Fig. 8. Variation of MF permeate flux with time.

$$\text{TOC removal } (\%) = \frac{\chi_{pw} - \chi_{rw}}{\chi_{pw}} \times 100 \quad (7)$$

where, χ_{pw} and χ_{rw} are the TOC in the PW and recovered water after EC, respectively.

The TOC removal is given on Table 4. As can be seen, the TOC removal increases from 17.9% to 29.3% as the current increases from 1 to 5 A. To obtain higher TOC removal, higher currents and longer reaction times were investigated. However, increasing the current above 8A for a reaction time of 20 min provided only a small increase in TOC removal. On the other hand, increasing reaction time and current leads to an increase in power costs. Consequently, all EC experiments consisted of treating 3 L of PW for 20 min using a current to 8A. The TOC in the treated PW that was the feed for MD was 64 mg L^{-1} as shown in Table 1.

3.4. MF performance

Fig. 8 shows the variation of permeate flux with time. Results are shown for two repeat runs. For the first run the initial flux was 28 L m^2 h^{-1}. The flux gradually decreased to 10 L m^2 h^{-1} after 320 min. The decrease in flux with time is due to the deposition of flocs on the membrane surface [39]. The membrane was regenerated and tested with a second batch of EC treated PW. The flux profile is very similar. The initial flux was 26 L m^2 h^{-1}. The result suggests that there is minimal irreversible fouling. We have used the same membrane with many different PW samples and have continued to regenerate the initial permeate by simply recirculating the DI water for 1 h on 10 occasions. The result suggests that EC was effective at flocculating the dissolved organic compounds and particle matter that could plug the pores of the MF membrane. A digital photo of the MF membrane after filtration is shown in Fig. S1A, and the MF membrane after regeneration with DI water is shown in Fig. S1B. It can be seen that most of the flocs that had adhered on the membrane surface were removed after circulating DI water for 1 h. SEM images of the unused and regenerated MF membranes are given in Fig. 9. As can be seen from Fig. 9A and B, most of the regenerated membrane appears to have an open structure similar to the structure of the unused membrane. This suggests that regenerating the MF membrane by circulating DI water is sufficient to remove flocs from the membrane surface resulting in minimal irreversible fouling. There were tiny pieces of residual floc left on the regenerated membrane, which was observed by SEM (shown in Fig. 9C). The gap between the flocs shows an open pore structure (Fig. 9D), which would have been occupied by the flocs before regeneration by DI water circulation. This further confirmed the pore structure was not irreversibly blocked by the flocs.

Particle floc size distribution (see supplementary data, Fig. S2) was

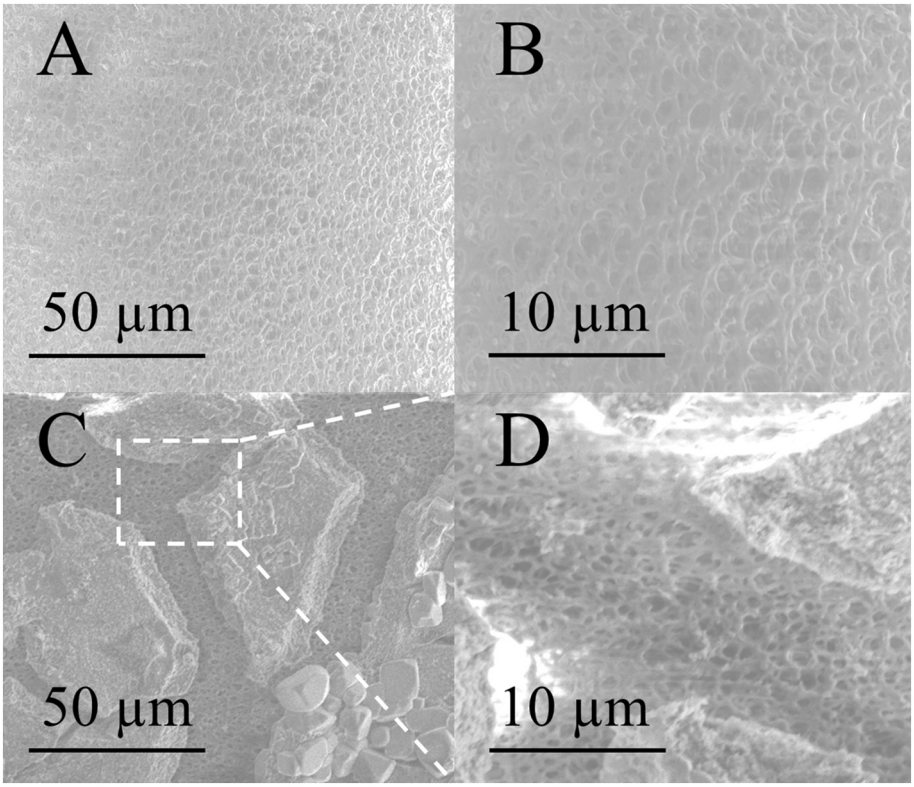

Fig. 9. SEM images of MF membranes: A and B) unused; C and D) specific area with flocs after regeneration.

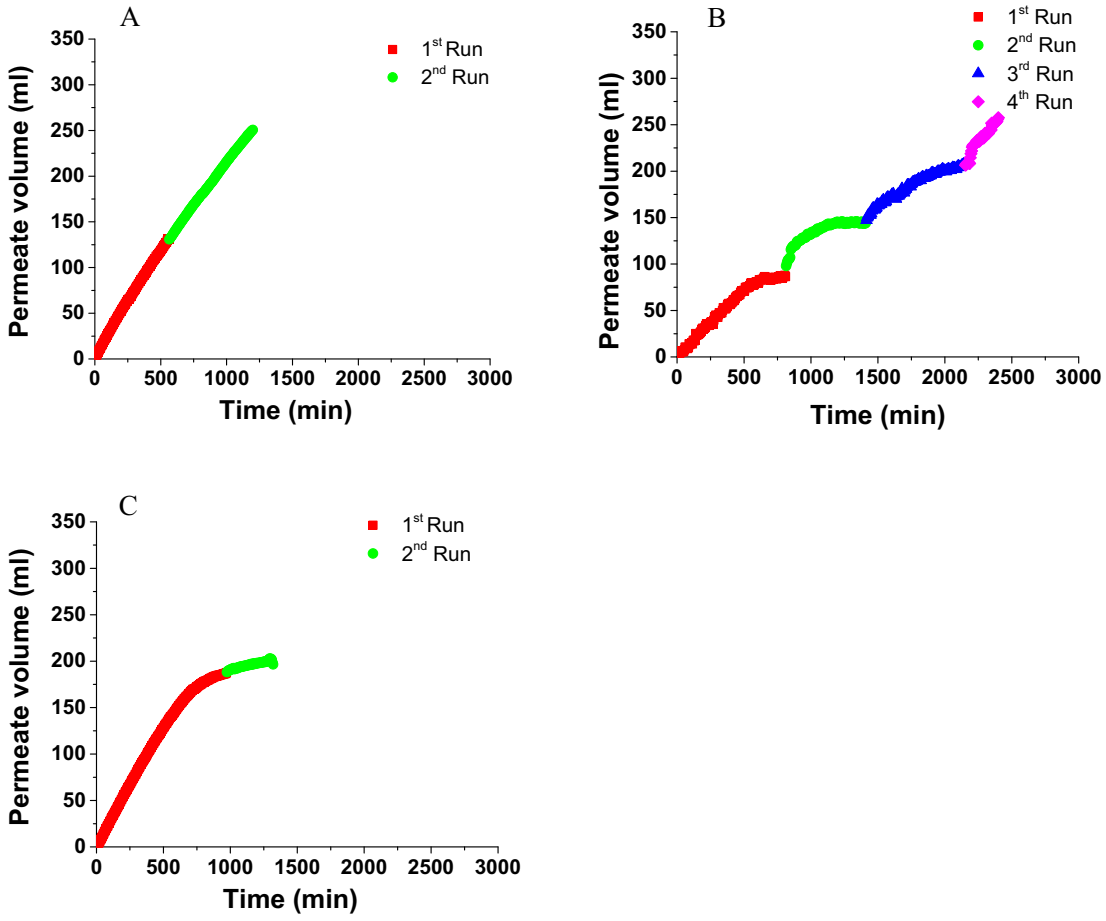

Fig. 10. Cumulative permeate volume versus time for the (A) commercial PVDF membrane, (B) electrospun PVDF-HFP membrane, (C) MWCNT PTFE membrane.

determined after EC for 20 min with an 8 A current using a Beckman Coulter (Indianapolis, IN) LS 13320 Laser Diffraction Particle Size Analyzer. Particle with a diameter larger than 0.1 μm, contributed to 97.6% of the total sludge volume (based on the cumulative volume percentage). Although 31.5% of the particles have a diameter smaller than 0.1 μm based on the number percentage, they represent only 2.4% volume of the fouling layer on the surface of the MF membrane. In fact, a cake layer may be formed very quickly by large size particles. Thus, most of the smaller particle will be rejected by the cake layer through size exclusion. This can help prevent small particles entering the membrane pores leading to irreversible pore blockage and fouling. The EDX result for the MF membrane (supplementary data Fig. S3) indicates that fouling may be mainly caused by $Al(OH)_3$, the major floc compound generated during EC.

3.5. MD performance

Fig. 10(A), (B) and (C) give the cumulative permeate volume versus time for the commercial PVDF membrane, the electrospun PVDF-HFP membrane and the MWCNT PTFE membrane, respectively. Fig. 11(A), (B) and (C) give the variation of permeate flux with permeate volume for the commercial PVDF membrane, the electrospun PVDF-HFP membrane and the MWCNT PTFE membrane, respectively. Table 5 summarizes the initial permeate flux and the volume of the feed water recovered for the three membranes.

As noted in Table 1 the feed TDS is 245,300 mg L^{-1} which is extremely high. The solubility of NaCl is around 360,000 mg L^{-1} at 30 °C [30,40]. We aim to recover 250 ml of permeate (30% water recovery) which would result in a feed TDS of 356,800 mg L^{-1}. Given the number of organic and inorganic compounds in the PW it is likely precipitation will occur at a TDS below 360,000 mg L^{-1}. The feed tank was kept at 36 °C while the temperature of the feed to the MD module was increased to 60 °C in order to minimize the risk of supersaturation and precipitation on the MD membrane. Precipitation was observed in the feed tank. Though the combined EC-MF pretreatment step reduced the TOC in the PW to around 44 mg L^{-1}, deposition of polar organic compounds on the membrane surface will increase the likelihood of precipitation of dissolved salts on this layer of adsorbed organic species.

Fig. 10(A) and Table 5 indicate that 131 ml of permeate were removed in the first run for the commercial PVDF membrane before the flux dropped to zero and the membrane was regenerated. The membrane was regenerated by simply running DI water on both sides of the membrane for 1 h. The flux for the second run was a little lower than the first run indicating some adsorbed species could not be removed by simply flushing the membrane with water. During the second run the desired total permeate volume of 250 ml was recovered.

The electrospun PVDF-HFP membrane behaved differently. Though the initial flux was similar to the commercial PVDF membrane, the flux dropped much more rapidly. In fact, the membrane had to be regenerated 3 times before the desired permeate volume of 250 ml was reached. As indicated in Figs. 10B, 11B and Table 5, for each subsequent run though the initial permeate flux was similar the rate of decrease of the flux was faster and the volume of recovered permeate was less. However, the membrane could be regenerated, and the conductivity was always less than 50 μS cm^{-1}.

The MWCNT PTFE membrane displayed the highest constant flux out of all three membranes during the first run. In fact, during the first run 186 ml of water were recovered. However, after regeneration the conductivity during the second run reached 50 μS cm^{-1} very quickly. In fact, it was not possible to recover 250 mL of permeate. The results indicate

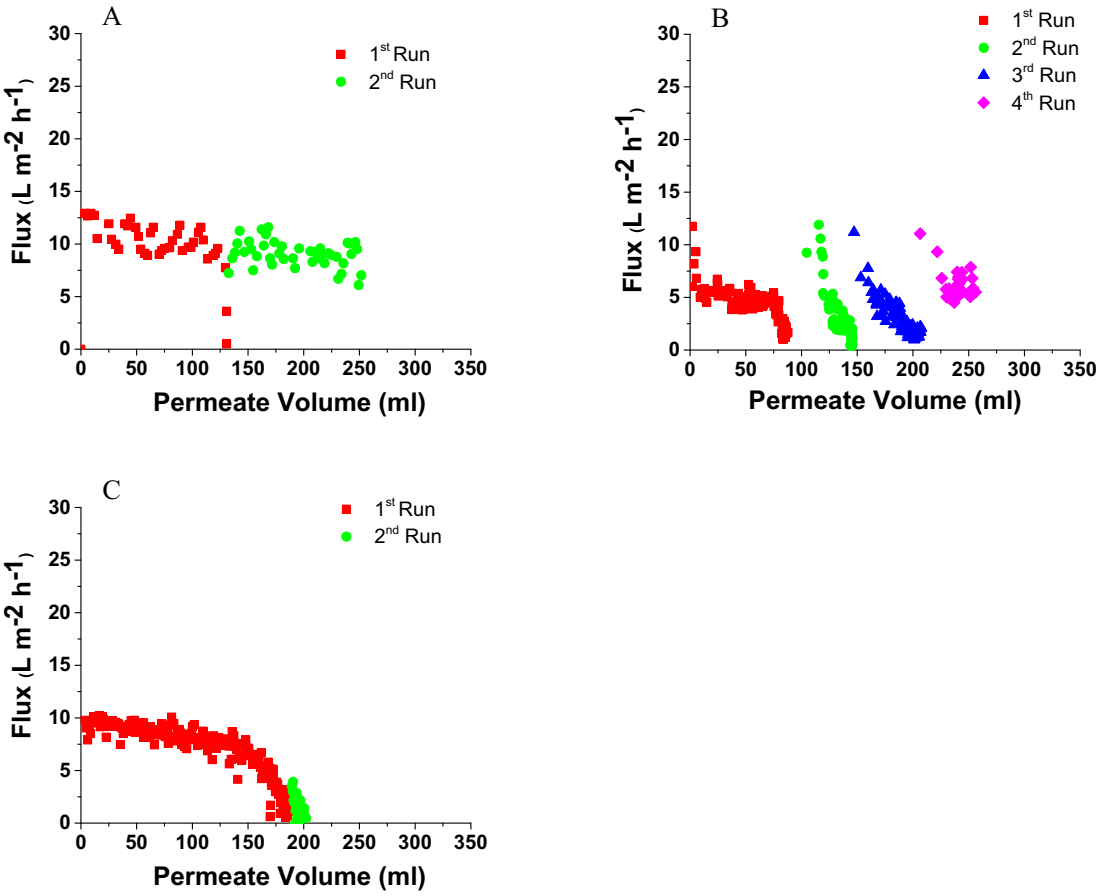

Fig. 11. Variation of permeate flux with permeate volume for (A) commercial PVDF membrane, (B) electrospun PVDF-HFP membrane, (C) MWCNT PTFE membrane.

Table 5
Summary of membrane performance results.

Membrane	Run 1 initial water flux (L m^{-2} h^{-1})	Run 1 water recovery (mL)	Run 2 initial water flux (L m^{-2} h^{-1})	Run 2 water recovery (mL)	Run 3 initial water flux (L m^{-2} h^{-1})	Run 3 water recovery (mL)	Run 4 initial water flux (L m^{-2} h^{-1})	Run 4 water recovery (mL)	Total water recovery (mL)
Commercial PVDF	13	131	10.0	121	–	–	–	–	252
Electrospun PVDF-HFP	12	87	12	59	11	56	11	50	252
MWCNT PTFE	10	186	4	17	–	–	–	–	203

the importance of membrane surface properties when treating real PW.

Table 2 indicates that the water contact angle for the commercial PVDF membrane is a little greater than the electrospun PVDF-HFP membrane, but the reverse is true for the oil contact angle. However, Table 3 indicates the increase in roughness for all three membranes after MD is significant. Thus, for all three membranes significant deposition occurs after MD. The oil contact angle of the MWCNT PTFE membrane is very low.

Our results indicate that a very low oil contact angle is undesirable if the PW contains dissolved organic compounds. The MWCNT membrane contains carbon nanotubes which provide channels for water vapor transport. Hence the membrane displays a much higher flux over a longer period of time which results in much greater water recovery during the first run before regeneration. Given the low oil contact angle, dissolved organic compounds can easily adsorbed onto the channels of carbon nanotubes, which leads to eventual flux decline. However, regeneration by flushing both sides of the membrane with DI water did not lead to release of the adsorbed foulants as evidenced by the low permeate flux at the start of the second run.

In MD, the feed is typically kept at the same temperature in both the feed tank and the MD cell. However as one approaches the solubility limit of the lest soluble components in the feed, scale formation on the membrane is likely [38]. In fact, both concentration and thermal polarization will provide a driving force for precipitation on the membrane surface. In order to maximize the water recovery and membrane life, we would like to promote precipitation in the feed reservoir, not the membrane surface.

Here, we cooled the feed reservoir relative to the temperature of the feed entering the MD module. Thus, we promoted precipitation in the feed reservoir but the least soluble component in the feed entered the MD module below its solubility limit due to the increases in temperature of the entering feed. Evidence of the fact that scale formation on the MD membrane was minimal is provided by EDX results (Fig. 7). No metallic elements were detected except for gold due to coating the samples. However, the change in C: F and O:F ratios given in Table 3 as well as the observed decline in flux indicate that fouling by organic compounds is significant [19,39]. Fluorine is present in all three membranes but not the PW (Table 1). After MD, the C/F ratios of the commercial PVDF,

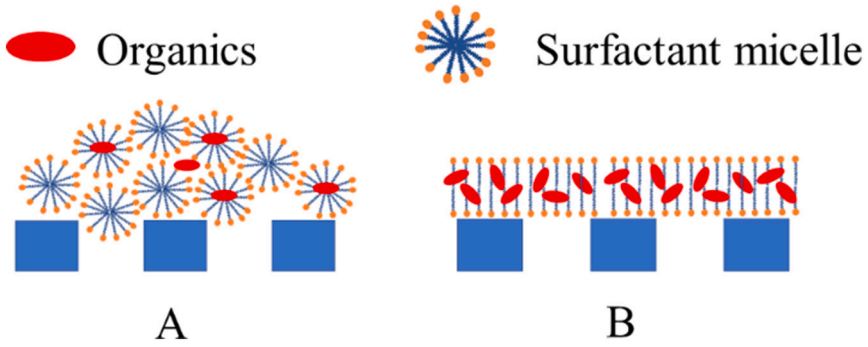

Fig. 12. Fouling layer caused by surfactant: A) micelle; B) bilayer.

electrospun PVDF-HFP, and MWCNT PTFE membranes have been increased by 52.0%, 44.1%, and 531.6%, respectively. As can be seen, the greatest increase in the C/F ratio was for the MWCNT PTFE membrane due to the adsorption of the organic compounds by the carbon nanotubes.

Hydrophobic and oleophobic surfaces will not suppress adsorption of low surface tension liquids as wetting by these liquid remains thermodynamically favorable [13]. Low surface tension compounds commonly found in PW include oils, alcohols and surfactants [7]. In addition as shown in Fig. 12, micelles can form in the feed solution once the concentrations of the surfactants exceeded their critical micelle concentration (CMC), which could lead to blockage of the membrane pores [41]. These micelles can grow from spherical aggregates to an elongated structures with an increase in concentration, which can lead to more severe fouling [42]. The proposed fouling mechanism is shown in Fig. 12A. There is also a chance of bilayer sheet formation on top of the membrane surface, as shown in Fig. 12B, leading to an increased roughness of the membrane as observed in the AFM images (Fig. 6(D), (E), and (F)).

Organic foulants (surfactant [43] and organic contaminants [44]) built up on the membrane surface during the MD forming an adsorbed layer. The presence of polar groups in the layer of deposited organic compounds can lead to scale formation on the adsorbed layer. This will lead to a decrease in permeate flux. Simply flushing both sides of the membrane with DI water may remove deposited scales but will be less effective at removing adsorbed organic compounds. Hence the flux is always lower after membrane regeneration. Given the very low oil contact angle for the MWCNT PTFE membrane as well as the much higher permeate flux, it is likely that adsorption of organic compounds was more rapid. In fact, during the second run the permeate conductivity increased above 50 μs cm^{-1}, indicating breakthrough of water through the membrane pores.

In this work we have attempted to recover water from an extremely high TDS PW. Under these challenging conditions we show that a combined EC-MF-MD process can recover water up to the solubility limit of NaCl. The concentration of $CaSO_4$ is around 677 mg L^{-1} in the PW (calculation based on sulfate present). Thus while $CaSO_4$ scale could form in this case, removal of 250 ml of permeate will not reach the solubility limit of $CaSO_4$ (>4000 mg L^{-1} with 1 mol/L NaCl) [45]. Further we show that a combined EC-MF-MD system where the feed reservoir is cooled relative to the feed entering the MD module will increase water recovery and move closer to a zero liquid discharge process. However, the energy cost will also be increased.

Here we have evaluated three different membrane structures. Our results suggest that simply optimizing the membrane surface properties is insufficient. It is important to consider the properties of the PW and the operating conditions. The MWCNT PTFE provided the highest flux and best performance as long as there are no organic compounds that can adsorb onto the membrane surface. On the other hand, the electrospun PVDF-HFP membrane appears to be easy to regenerate. AFM mad SEM images appear to show less absorption on the nanofibers. In reality it is unlikely a single membrane will be used to concentrate the reject from a low TDS to above the solubility limit of the salts present. A staged process with inter-stage heat exchange is more likely. In addition, one can optimize the membrane for the TDS of the stage. Our future work will focus on development of an EC-MF-MD process that could be used to treat at a side stream at a hydraulic fracturing facility.

4. Conclusion

We have investigated a combined EC-MF-MD process for treating hydraulic fracturing PW. The PW investigated here had a TDS of 245,300 mg L^{-1}. Nevertheless, the process developed here could concentrate the reject to the solubility limit of the dissolved salts. By reducing the temperature of the feed tank to 36 °C while the temperature of the feed entering the MD module was maintained at 60 °C precipitation on the membrane is suppressed and occurs in the feed tank. We show that EC can lead to adequate reduction in the PW TOC (67 mg L^{-1}) and MF can efficiently remove the particulate matter. The stability of the MD membrane is critical. Three different membranes with different surface properties were tested. An ideal membrane is one which provides a high flux at high TDS and is resistant to breakthrough. It is likely that ideal membrane will depend on the TDS and other properties of the PW.

Declaration of competing interest

The authors declare that they have no known competing financial interests or personal relationships that could have appeared to influence the work reported in this paper.

Acknowledgements

Funding for this work was provided by the Arkansas Research Alliance, National Science Foundation through (a) Industry/University Cooperative Research Center for Membrane Science, Engineering and Technology, (IIP 1822101, 1913839 1930079), (b) Research Experiences for Undergraduates REU Site: From Bench to Market: Engineering Systems for High Efficiency Separations (EEC 1659653) and the University of Arkansas. The authors gratefully acknowledge the financial support from the RAPID Manufacturing Institute, a public-private partnership between the Advanced Manufacturing Office (AMO) of the US Department of Energy and the American Institute of Chemical Engineers (AIChE) under the subaward DE-EE0007888-08-08.

Appendix A. Supplementary data

Supplementary data to this article can be found online at https://doi.org/10.1016/j.desal.2020.114886.

References

[1] J. Pichtel, Oil and gas production wastewater: soil contamination and pollution prevention, Applied and Environmental Soil Science 2016 (2016) 1–24.
[2] D.S. Alessi, A. Zolfaghari, S. Kletke, J. Gehman, D.M. Allen, G.G. Goss, Comparative analysis of hydraulic fracturing wastewater practices in unconventional shale development: water sourcing, treatment and disposal practices, Canadian Water Resources Journal/Revue canadienne des ressources hydriques 42 (2) (2017) 105–121.
[3] A. Carrero-Parreño, V.C. Onishi, R. Salcedo-Díaz, R. Ruiz-Femenia, E.S. Fraga, J. A. Caballero, J.A. Reyes-Labarta, Optimal pretreatment system of flowback water from shale gas production, Ind. Eng. Chem. Res. 56 (15) (2017) 4386–4398.
[4] H. Chen, K.E. Carter, Water usage for natural gas production through hydraulic fracturing in the United States from 2008 to 2014, J. Environ. Manag. 170 (2016) 152–159.
[5] G. Chen, Z. Wang, L.D. Nghiem, X.-M. Li, M. Xie, B. Zhao, M. Zhang, J. Song, T. He, Treatment of shale gas drilling flowback fluids (SGDFs) by forward osmosis: membrane fouling and mitigation, Desalination 366 (2015) 113–120.
[6] A. Vengosh, N. Warner, R. Jackson, T. Darrah, The effects of shale gas exploration and hydraulic fracturing on the quality of water resources in the United States, Procedia Earth and Planetary Science 7 (2013) 863–866.
[7] R. Barati, J.-T. Liang, A review of fracturing fluid systems used for hydraulic fracturing of oil and gas wells, Journal of Applied Polymer Science 131 (16) (2014) n/a-n/a.
[8] K.B. Gregory, R.D. Vidic, D.A. Dzombak, Water management challenges associated with the production of shale gas by hydraulic fracturing, Elements 7 (3) (2011) 181–186.
[9] R.F.B. Becker, Produced and Process Water Recycling Using Two Highly Efficient Systems to Make Distilled Water, SPE Annual Technical Conference and Exhibition, Society of Petroleum Engineers, Dallas, Texas, 2000, p. 10.
[10] E. Mohammad-Pajooh, D. Weichgrebe, G. Cuff, B.M. Tosarkani, K.-H. Rosenwinkel, On-site treatment of flowback and produced water from shale gas hydraulic fracturing: a review and economic evaluation, Chemosphere 212 (2018) 898–914.
[11] M. Sadrzadeh, J. Hajinasiri, S. Bhattacharjee, D. Pernitsky, Nanofiltration of oil sands boiler feed water: effect of pH on water flux and organic and dissolved solid rejection, Sep. Purif. Technol. 141 (2015) 339–353.
[12] K. Jepsen, M. Bram, S. Pedersen, Z. Yang, Membrane fouling for produced water treatment: a review study from a process control perspective, Water 10 (7) (2018) 847.
[13] A. Deshmukh, C. Boo, V. Karanikola, S. Lin, A.P. Straub, T. Tong, D.M. Warsinger, M. Elimelech, Membrane distillation at the water-energy nexus: limits, opportunities, and challenges, Energy Environ. Sci. 11 (5) (2018) 1177–1196.
[14] M. Rebhun, M. Lurie, Control of organic matter by coagulation and floc separation, Water Sci. Technol. 27 (11) (1993) 1–20.
[15] E. Butler, Y.-T. Hung, R.Y.-L. Yeh, M. Suleiman Al Ahmad, Electrocoagulation in Wastewater Treatment, Water 3 (2) (2011) 495–525.
[16] J.E. Bryant, J. Haggstrom, An Environmental Solution to Help Reduce Freshwater Demands and Minimize Chemical Use, SPE/EAGE European Unconventional Resources Conference and Exhibition, Society of Petroleum Engineers, Vienna, Austria, 2012, p. 10.
[17] B.M. Todd, D.C. Kuykendall, M.B. Peduzzi, J. Hinton, Hydraulic Fracturing-Safe, Environmentally Responsible Energy Development, SPE E&P Health, Safety, Security and Environmental Conference-Americas, Society of Petroleum Engineers, Denver, Colorado, USA, 2015, p. 12.
[18] K. Sardari, P. Fyfe, D. Lincicome, S. Ranil Wickramasinghe, Combined electrocoagulation and membrane distillation for treating high salinity produced waters, J. Membr. Sci. 564 (2018) 82–96.
[19] K. Sardari, P. Fyfe, D. Lincicome, S.R. Wickramasinghe, Aluminum electrocoagulation followed by forward osmosis for treating hydraulic fracturing produced waters, Desalination 428 (2018) 172–181.
[20] K. Sardari, P. Fyfe, S. Ranil Wickramasinghe, Integrated electrocoagulation – forward osmosis – membrane distillation for sustainable water recovery from hydraulic fracturing produced water, J. Membr. Sci. 574 (2019) 325–337.
[21] M.S. El-Bourawi, Z. Ding, R. Ma, M. Khayet, A framework for better understanding membrane distillation separation process, J. Membr. Sci. 285 (1) (2006) 4–29.
[22] J. Phattaranawik, R. Jiraratananon, A.G. Fane, Heat transport and membrane distillation coefficients in direct contact membrane distillation, J. Membr. Sci. 212 (1) (2003) 177–193.
[23] B.B. Ashoor, S. Mansour, A. Giwa, V. Dufour, S.W. Hasan, Principles and applications of direct contact membrane distillation (DCMD): a comprehensive review, Desalination 398 (2016) 222–246.
[24] I. Metcalf, G. Eddy, F. Tchobanoglous, H.D. Burton, Stensel, Wastewater Engineering: Treatment and Reuse, McGraw-Hill Education, 2002.
[25] Z. Anari, A. Sengupta, K. Sardari, S.R. Wickramasinghe, Surface modification of PVDF membranes for treating produced waters by direct contact membrane distillation, Sep. Purif. Technol. 224 (2019) 388–396.
[26] S. Ramakrishna, K. Fujihara, W.-E. Teo, T. Yong, Z. Ma, R. Ramaseshan, Electrospun nanofibers: solving global issues, Mater. Today 9 (3) (2006) 40–50.
[27] M.K. Au-Leach, Z.-Q. Au-Feng, S.J. Au-Tuck, J.M. Au-Corey, Electrospinning fundamentals: optimizing solution and apparatus parameters, JoVE 47 (2011) e2494.
[28] N. Wang, T. Wang, Y. Hu, Tailoring membrane surface properties and ultrafiltration performances via the self-assembly of polyethylene glycol-block-polysulfone-block-polyethylene glycol block copolymer upon thermal and solvent annealing, ACS Appl. Mater. Interfaces 9 (36) (2017) 31018–31030.
[29] K. Smolders, A.C.M. Franken, Terminology for membrane distillation, Desalination 72 (3) (1989) 249–262.
[30] M. Malmali, P. Fyfe, D. Lincicome, K. Sardari, S.R. Wickramasinghe, Selecting membranes for treating hydraulic fracturing produced waters by membrane distillation, Sep. Sci. Technol. 52 (2) (2017) 266–275.
[31] T.C. Timmes, H.-C. Kim, B.A. Dempsey, Electrocoagulation pretreatment of seawater prior to ultrafiltration: pilot-scale applications for military water purification systems, Desalination 250 (1) (2010) 6–13.
[32] P. Cañizares, C. Jiménez, F. Martínez, C. Sáez, M.A. Rodrigo, Study of the electrocoagulation process using aluminum and iron electrodes, Ind. Eng. Chem. Res. 46 (19) (2007) 6189–6195.
[33] K. Sardari, J. Askegaard, Y.-H. Chiao, S. Darvishmanesh, M. Kamaz, S. R. Wickramasinghe, Electrocoagulation followed by ultrafiltration for treating poultry processing wastewater, Journal of Environmental Chemical Engineering 6 (4) (2018) 4937–4944.
[34] M. Kamaz, A. Sengupta, A. Gutierrez, Y.H. Chiao, R. Wickramasinghe, Surface modification of PVDF membranes for treating produced waters by direct contact membrane distillation, Int. J. Environ. Res. Public Health 16 (5) (2019).
[35] C. Boo, J. Lee, M. Elimelech, Omniphobic polyvinylidene fluoride (PVDF) membrane for desalination of shale gas produced water by membrane distillation, Environ Sci Technol 50 (22) (2016) 12275–12282.
[36] M. Nasrullah, L. Singh, Z. Mohamad, S. Norsita, S. Krishnan, N. Wahida, A. W. Zularisam, Treatment of palm oil mill effluent by electrocoagulation with presence of hydrogen peroxide as oxidizing agent and polialuminum chloride as coagulant-aid, Water Resources and Industry 17 (2017) 7–10.
[37] M. Asselin, P. Drogui, H. Benmoussa, J.-F. Blais, Effectiveness of electrocoagulation process in removing organic compounds from slaughterhouse wastewater using monopolar and bipolar electrolytic cells, Chemosphere 72 (11) (2008) 1727–1733.
[38] F. Edwie, T.-S. Chung, Development of simultaneous membrane distillation–crystallization (SMDC) technology for treatment of saturated brine, Chemical Engineering Science 98 (2013) 160–172.
[39] M. Changmai, M. Pasawan, M.K. Purkait, Treatment of oily wastewater from drilling site using electrocoagulation followed by microfiltration, Sep. Purif. Technol. 210 (2019) 463–472.
[40] M.R.J. Daelman, E.M. van Voorthuizen, U.G.J.M. van Dongen, E.I.P. Volcke, M.C. M. van Loosdrecht, Methane emission during municipal wastewater treatment, Water Res. 46 (11) (2012) 3657–3670.
[41] N.G.P. Chew, S. Zhao, C.H. Loh, N. Permogorov, R. Wang, Surfactant effects on water recovery from produced water via direct-contact membrane distillation, J. Membr. Sci. 528 (2017) 126–134.
[42] B. Kronberg, K. Holmberg, B. Lindman, Surface Chemistry of Surfactants and Polymers, John Wiley & Sons, United Kingdom, 2014.
[43] Y. Kaya, C. Aydiner, H. Barlas, B. Keskinler, Nanofiltration of single and mixture solutions containing anionics and nonionic surfactants below their critical micelle concentrations (CMCs), J. Membr. Sci. 282 (1–2) (2006) 401–412.
[44] P. Xu, J.E. Drewes, T.-U. Kim, C. Bellona, G. Amy, Effect of membrane fouling on transport of organic contaminants in NF/RO membrane applications, J. Membr. Sci. 279 (1–2) (2006) 165–175.
[45] E. Bock, On the solubility of anhydrous calcium sulphate and of gypsum in concentrated solutions of sodium chloride at 25°C, 30°C, 40°C, and 50°C, Can. J. Chem. 39 (9) (1961) 1746–1751.